Chapter 7
Estimation of Nutrient and Suspended Sediment Loads in the Ishikari River

7.1 Introduction

The importance of surface water quality in controlling the health of aquatic ecosystems, affecting drinking water resources, and human health is increasingly recognized. Nutrients (mainly nitrogen and phosphorus) are essential for the life of animals and plants, but high concentrations cause many ecological problems (Carpenter et al. 1998; Li e 2011; Smith 1982; Sprague and Lorenz 2009). Excessive sediments reduce water quality, which has negative impacts on material fluxes, aquatic geochemistry, water quality, and channel morphology (Dedkov and Mozzherin 1992; Ishida et al. 2010; Meade et al. 1985). In order to effectively manage and protect water resources, it is important to understand nutrients and sediments dynamics (Gruber and Galloway 2008; Sprague and Lorenz 2009). Concentrations and loads of nutrients and SS are usually estimated based on models and infrequent monitoring data (Armour et al. 2009; Kulasova et al. 2012; Li et al. 2009, 2011; Ma et al. 2011). River flow data, usually obtained from sparse monitoring stations, provides the basis for estimating critical water quality components, as the concentration and load of these components typically change naturally with changes in flow. In addition, it is often difficult to obtain water-quality records representing the concentration of components in a rapidly changing water stream over a long period of time (years to decades). Therefore, the uncertainty of the composition load estimate is often high (Christensen et al. 2000; Reckhow 1994).

Japan's efforts in water management have greatly improved the estimation of water quality (Duan et al. 2013; Wang et al. 2016). For example, a national data collection network called "National Land Water Information" (http://www1.river.go.jp/) was built to offer reliable and real-time water data including river discharges, water quality, and precipitation. Since the load estimation process is complicated by the transformation bias (Ferguson 1986; Webb et al. 1997), data censoring (Gilbert 1987), and non-normality (Helsel and Hirsch 1992; Shumway et al. 2002), there is usually a bias in the estimated load of the model simulation (Johnes 2007). Meanwhile, in Japan, high suspended sediment load is increasingly recognized as an important issue

W. Duan and K. Takara, *Impacts of Climate and Human Activities on Water Resources and Quality*, https://doi.org/10.1007/978-981-13-9394-5_7

in river basin management (Mizugaki et al. 2008; Somura et al. 2012). For example, the Ishikari River Basin has long been plagued by heavy suspended sediment loads, which often result in high turbidity and riverbed erosion along rivers, including the economic and government center (e.g., Sapporo) of Hokkaido. A few studies have focused on the SS management in the Ishikari River Basin. For example, Asahi et al. (2003) argued that it is necessary to directly deal with the influence of tributaries, and the sediment discharged from the tributaries contributes to the discharge of sediment from the estuary. However, the detailed sediment sources and transportation in the Ishikari River Basin is still poorly understood.

Therefore, it is important to improve estimation methods for obtaining reliable water quality loads. Based on the Maintenance of Variance-Extension type 3 (MOVE.3) and the regression model Load Estimator (LOADEST), this chapter firstly estimated total nitrogen (TN), total phosphorus (TP), and suspended sediments (SS) loads at five sites on the Ishikari River, Japan, from January 1985 to December 2010. Then, this chapter developed a spatially explicit, regional empirical model of suspended sediments (SS, soil, and other particulate matter) for the whole Ishikari River Basin. This model is used to analyze the source and transport process of the SS. The ultimate goal of this work is to provide information and tools to help resource managers identify priority sources of pollution and reduce pollution to protect water resources and protect aquatic ecosystems in the Ishikari River Basin.

7.2 Study Area and Datasets

7.2.1 Study Area and Data Collection

Figure 7.1 shows that the Ishikari River Basin is located in the middle of Hokkaido with a total drainage area of 14,330 km^2. The Ishikari River originates from Mt. Ishikaridake (elev. 1967 m) in the Taisetsu Mountains of central Hokkaido, and flows southward into flows south into the vast Ishikari Plain and finally flows into the Sea of Japan. The length of the Ishikari River mainstream is 268 km, ranking third in Japan. At the Sapporo weather station (elev. 17 m), the monthly temperature of the warmest month (August) is about 22.0 °C, and the monthly temperature of the coldest month (January) is about −4.1 °C.

As shown in Fig. 7.1, 31 monitoring stations were selected in this chapter. Of them, 5 monitoring stations including station 7, station 10, station 17, station 20, and station 31 were used to do the trend analysis. The sites Yinou-oohashi, Yiwamizawa-oohashi, and Yishikarikakou-bashi are located in the upper, middle, and lower reaches of the mainstream, respectively, while the Akane-bashi and Umaoyi-bashi sites are located in the tributaries of Uryū and Yūbari, respectively. Typically, each site was measured and collected for water quality concentration (TN, TP, and SS) and river discharges per one month or two months from 1985 to 2010 by the National Land with Water Information (http://www1.river.go.jp/) monitoring network. A total number

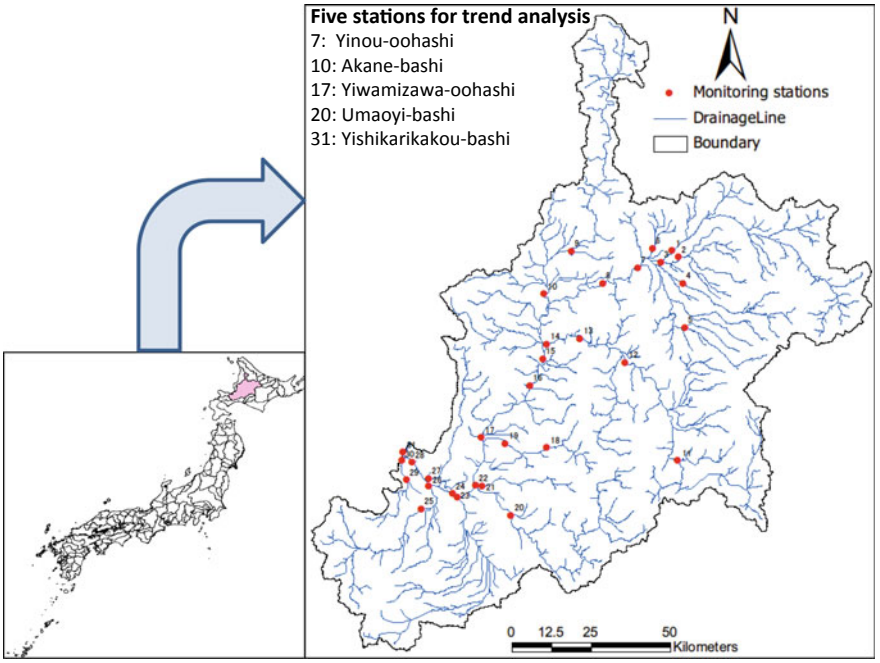

Fig. 7.1 Study area and monitoring stations for the Ishikari River

of 312 samples for each testing parameter were collected at Akane-bashi, Yinouo-ohashi, and Umaoyi-bashi stations, and 274 samples were collected for each testing parameter at Yiwamizawa-oohashi and Yishikarikakou-bashi stations. All these 31 monitoring stations were used to calibrate the SS model for the Ishikari River Basin.

7.3 Statistical Methods

7.3.1 Streamflow Extension

Based on daily streamflow values recorded at nearby and hydrologically similar index stations, a streamflow record extension method called the Maintenance of Variance-Extension type 3 (MOVE.3) (Vogel and Stedinger 1985) was applied to estimate missing flow values or to extend the record at a short-record station. The method can be expressed by the following equation:

$$Y_i = \beta X_i + b + e_i \tag{7.1}$$

where Y_i represents the logarithm of the river discharge for the ith day at the short-record station; X_i represents the logarithm of the river discharge for the ith day at the long-record station, β represents the slope of the regression-line, b represents the intercept of the regression-line, e_i represents the difference between the estimated regression-line and the measured Y value for the ith measurement.

7.3.2 Loads Estimation

In theory, based on constituent concentration (C) and discharge (Q), the SS or chemical constituent load ($\emptyset$) can be computed using the following equation:

$$\emptyset = \int C(t)Q(t)\mathrm{d}t \tag{7.2}$$

where t is the time period. In Eq. 7.2, the calculation needs a continuous record of concentration and discharge when estimating the SS or chemical constituent load ($\emptyset$). Although it is easy to measure river discharges at a sufficiently high frequency, it is often difficult to obtain continuous water quality data due to the expense of collecting and analyzing samples. Therefore, Eq. 7.2 could be expressed as follows:

$$L_T = \Delta t \sum_{i=1}^{n} L_i \tag{7.3}$$

where L_T represents an estimate of total water quality load, L_i represents an estimate of instantaneous water quality load, n represents the number of discrete points in time, and Δt represents the time interval represented by the instantaneous water quality load.

Then, we have calibrated the above regression model using the FORTRAN Load Estimator (LOADEST) (Runkel et al. 2004). Four statistical estimation methods including the adjusted maximum likelihood estimation (AMLE), maximum likelihood estimation (MLE), linear attribution method (LAM), and least absolute deviation (LAD) were provided in the LOADEST when carrying out the calibration procedures. Of them, when the model calibration errors (residuals) are normally distributed, both AMLE and MLE are suitable, but AMLE is the more appropriate method when containing censored data (i.e., when data are reported as less than or greater than some threshold). Other two methods including LAM and LAD are the appropriate methods when the residuals are not normally distributed. Therefore, since the input data in this chapter included censored data and the model calibration residuals were normally distributed within acceptable limits, the AMLE estimation method was chosen to calibrate at each monitoring station. The output regression model equations can be expressed as follows (Runkel et al. 2004):

$$\ln(L_i) = a + b\ln Q + c\ln Q^2 + d\sin(2\pi\, dtime) + e\cos(2\pi\, dtime) + f\, dtime + g\, dtime^2 + \varepsilon \tag{7.4}$$

where L_i represents the calculated water quality load for the sample i, Q represents the stream discharge; $dtime$ represents the time, in decimal years from the beginning of the calibration period, ε represents the error, and a, b, c, d, e, f, g represent the fitted parameters in the multiple regression model of water quality loads. According to the lowest Akaike information criterion (AIC) values, some of the regression equations did not contain all terms (Sakamoto et al. 1986). The AIC could be calculated as follows:

$$AIC = 2n - 2\ln(L) \tag{7.5}$$

where n represents the number of parameters in the statistical water quality model and L represents the maximized value of the likelihood function for the estimated water quality model. The monthly and seasonal average TN, TP, and SS loads were estimated based on the above formula. Four seasons were considered as follows: winter (December, January, February), spring (March, April, May), summer (June, July, August), and autumn (September, October, November).

7.3.3 Trend Analysis

The Mann–Kendall test was employed to compute trends of water quality in Ishikari River Basin, which is a nonparametric rank-based statistical test (Kendall 1975; Mann 1945) and has been used to analyze trends in hydro-meteorological time series (Duan et al. 2017; Yue et al. 2002). For independent and randomly ordered on a time series $X_i\{X_i, i = 1, 2, \ldots, n\}$, the null hypothesis H_0 in Mann–Kendall test assumes that there is no trend and this is tested against the alternative hypothesis H_1, which assumes that there is a trend. The Mann–Kendall S Statistic is computed as follows:

$$S = \sum_{i=1}^{n-1} \sum_{j=i+1}^{n} \operatorname{sign}\left(T_j - T_i\right) \tag{7.6}$$

$$\operatorname{sign}\left(T_j - T_i\right) = \begin{cases} 1 & \text{if } T_j - T_i > 0 \\ 0 & \text{if } T_j - T_i = 0 \\ -1 & \text{if } T_j - T_i < 0 \end{cases} \tag{7.7}$$

where T_j and T_i are the water quality (TN, TP, and SS loads) variability at multiple time scales j and i, $j > i$, respectively. When $n \geq 10$, the statistic S is approximately normally distributed with the mean and variance as follows:

$$E(S) = 0 \tag{7.8}$$

The variance (σ^2) for the S-statistic is defined by

$$\sigma^2 = \frac{n(n-1)(2n+5) - \sum t_i(i)(i-1)(2i+5)}{18} \tag{7.9}$$

where t_i denotes the number of ties to extent i. The summation term in the numerator is used only if the water quality (TN, TP, and SS loads) data contains tied values. The standard test statistic Z_S is calculated as follows:

$$Z = \begin{cases} \frac{S-1}{\sigma} & \text{for } S > 0 \\ 0 & \text{for } S = 0 \\ \frac{S+1}{\sigma} & \text{for } S < 0 \end{cases} \tag{7.10}$$

The test statistic Z_S is used as a measure of significance of trend of the water quality (TN, TP, and SS loads) (e.g., Yue et al. 2002). This test statistic is used to test the null hypothesis (H_0). That is, if $|Z_S|$ is great than $Z_{\alpha/2}$, where α is the chosen significance level (e.g., 5% with $Z_{0.025} = 1.96$) then the null hypothesis is invalid implying that the trend of water quality (TN, TP, and SS loads) is significant.

7.4 Modeling Tools

7.4.1 SPARROW Model

Computer-based modeling is essential for organizing and understanding complex data related to water quality conditions and for developing management strategies and decision support tools for water resource managers (Somura et al. 2012). There are lots of hydrological and water quality models to describe and identify sources of pollutants and transportations at various spatial scales (e.g., HSPF (Jeon et al. 2011; Johanson et al. 1980), ANSWERS (Beasley et al. 1980), SWAT (Kirsch et al. 2002; Liew et al. 2012), and ANN (Rajaee et al. 2011)). Nowadays, the GIS-based watershed model SPARROW (SPAtially Referenced Regression On Watershed attributes) is very popular and widely used to evaluate the water quality in the United States (Smith et al. 1997; Alexander et al. 2000, 2007; Duan et al. 2012, 2015; McMahon et al. 2003). Figure 7.2 shows the functional linkages between the major spatial components of SPARROW models. Monitoring station flux estimates are long-term flux estimates used as response variables in the model. The flux estimates for the monitoring station are derived from a station-specific model that correlates the concentration of contaminants in each water sample with a continuous record of the water flow time series. Generally, a nonlinear least-squares multiple regression is used to describe and estimate the relationship between spatially referenced basin and channel characteristics (predictors) and in-stream water pollution loads (response) (Schwarz et al.

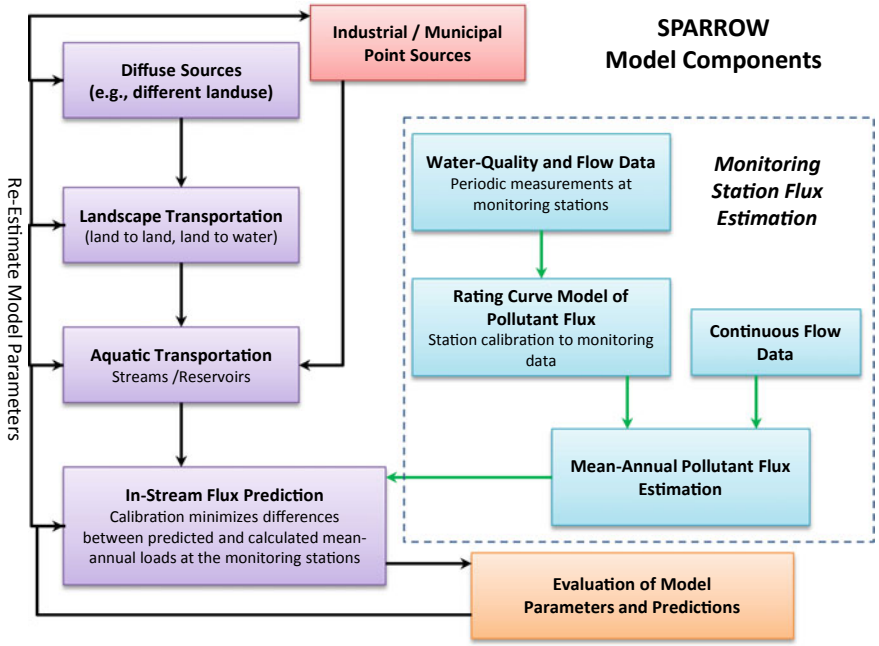

Fig. 7.2 Schematic of the major SPARROW model components (From Schwarz et al. 2006)

2006). This function can track the transportation of water quality to evaluate the pollutants' supply and attenuation in streams and reservoirs (Preston and US 2009).

The fundamental principle of SPARROW modeling can be expressed as follows (Alexander et al. 2007):

$$F_i^* = \left[\left(\sum_{j \in J(i)} F_j' \right) A\left(Z_i^S, Z_i^R; \theta_S, \theta_R\right) + \left(\sum_{n=1}^{N_S} S_{n,i} \alpha_n D_n \left(Z_i^D; \theta_D\right) \right) A'\left(Z_i^S, Z_i^R; \theta_S, \theta_R\right) \right] \varepsilon_i \tag{7.11}$$

The first summation term $\left(\left(\sum_{j \in J(i)} F_j' \right) A\left(Z_i^S Z_i^S \theta_S \theta_R\right) \right)$ is the suspended sediments flux that leaves upstream reaches and is delivered downstream to reach i, where F_j' represents the measured suspended sediment flux $\left(F_j^M\right)$ when upstream reach j is monitored and equals the given model-estimated flux (F_j^*) when it is not. $A(\cdot)$ represents the stream delivery function, which indicates suspended sediment loss processes acting on flux as it travels along the reach pathway. In other words, it defines the fraction of suspended sediment flux entering reach i at the upstream node that is delivered to the downstream node. Z^S and Z^R are functions of measured

stream and reservoir characteristics in the Ishikari River Basin, respectively, and θ_S and θ_R are the corresponding coefficient vectors.

The second summation term represents the amount of suspended sediment flux introduced to the stream network at reach i in Ishikari River Basin, which consists of the flux originating from specific suspended sediment sources in the basin, indexed by $n = 1, 2, \ldots, N_S$. Each suspended sediment source has a source variable, denoted as S_n, with the corresponding source-specific coefficient (α_n). The function $D_n(\cdot)$ is the land-to-water delivery factor, which means the suspended sediment source is transported from the land to the water. The land-to-water delivery factor is denoted by Z_i^{θ}, which is a source-specific function of a vector of delivery variables, with an associated vector of coefficients (θ_D). The function $A'(\cdot)$ is the fraction of flux originating in and delivered to reach i, which is transported to the downstream node in the river network. The sediment introduced to the reach from its incremental drainage area receives the square root of the full in-stream delivery when the reach i is classified as a stream (as opposed to a reservoir reach). This assumption means that suspended sediments are introduced to the reach network at the midpoint of reach i and thus are subjected to only half of the time of arrival. In addition, for a section classified as a reservoir, we assume that the suspended sediment mass will receive the full attenuation defined for the reach. ε_i is the multiplicative error term, which is considered to be independent and evenly distributed across separate sub-basins in the intermediate drainage system between stream monitoring stations.

The suspended sediment loss in streams is modeled according to a first-order decay process. In this process, the sediment mass fraction derived from the upstream node and transported along the reach i to the downstream node is estimated as a continuous function of the mean water time of travel (T_i^S; units of time) and average water depth (D_i) in reach i. The process can be expressed as follows:

$$A\left(Z_i^S, Z_i^R; \theta_S, \theta_R\right) = \exp\left(-\theta_S \frac{T_i^S}{D_i}\right) \tag{7.12}$$

where θ_S is an estimated suspended sediment mass-transfer flux-rate coefficient in units of length time^{-1}. The rate coefficient is independent of the amount of water that is proportional to the amount of water, such as streamflow and depth (3). Based on the average water depth, the rate can be re-expressed as a reaction rate coefficient (time^{-1}).

7.4.2 Input Data

In this study, the input data used to construct the SPARROW model is divided into: (1) stream network data to define the watershed and catchment area in the Ishikari River Basin; (2) The suspended sediment loading data from many monitoring

Table 7.1 Summary of input data and calibration parameters

Category	Input data	Data source
The stream network	Stream network, stream lengths, sub-catchment boundaries, sub-catchment areas	Automated catchment delineation based on a 50 m DEM, with modification flow diversions
Stream load data	Monitoring station	The suspended sediment flux at 31 stations from 1982 to 2010 was obtained from the National Land with Water Information monitoring network
Sediment source data	Developing land, forest land, agricultural land, and water land	Land-use data were downloaded from the Ministry of Land, Infrastructure, Transport and Tourism, Japan, 2006
Environmental setting data	Mean annual precipitation	The 20-year (1990–2010) average from Japanese Meteorological Agency
	Catchment slope	Mean value of local slope, obtained from 50 m DEM
	Soil texture, soil permeability	Obtained from the 1:5.000.000-scale FAO/UNESCO Soil Map of the World and the National and Regional Planning Bureau, Japan
	Reservoir (dam) loss	The Japan Dam Foundation (http://damnet.or.jp/)

stations within the model boundary (dependent variable); (3) Sediment source data describing the source of all modeled sediments or other components (independent variables); (4) Environmental datasets describing the environmental settings of the modeled, which cause statistically in the amphibious transport of sediments (independent variables). The input datasets are described in more detail in Table 7.1.

7.4.2.1 The Stream Network

Figure 7.3 shows the hydrologic network and catchments used for the SPARROW model of the Ishikari River basin, which are obtained from a 50 m digital elevation model (DEM). In total, there were 900 stream reaches, each with an associated sub-catchment. River networks mainly include river arrival and sub-catchment characteristics, such as river length, water flow direction, reservoir characteristics (such as surface area), and local and total drainage areas. For example, the areas of the smallest sub-catchment are 0.009 km^2, and the largest one is 117 km^2. The median area for these sub-catchments is 15.9 km^2.

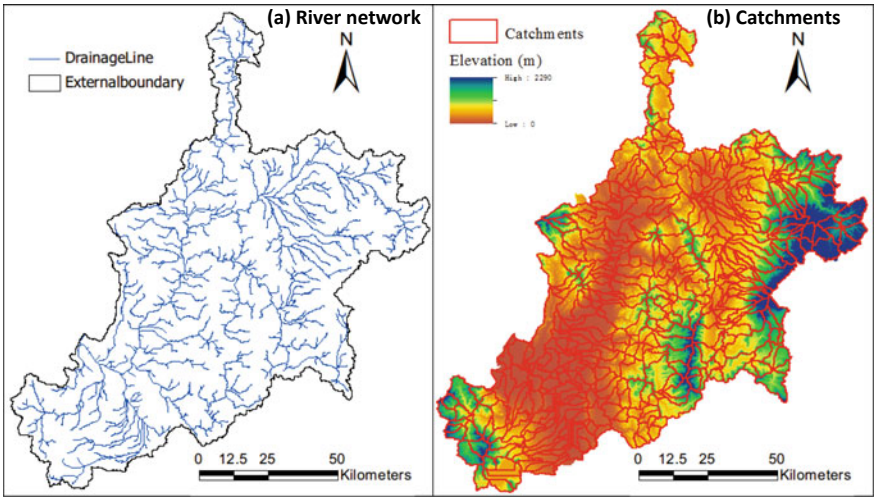

Fig. 7.3 Schematic showing **a** the river network and **b** 900 catchments in the Ishikari River Basin

7.4.2.2 Stream Load Data

Thirty-one stations (see Fig. 7.1) were selected for model calibration. The SS concentration and daily flow data for each station from 1982 to 2010 were collected through the National Land Water Information (http://www1.river.go.jp/) monitoring network. However, some flow measurement stations have very short recording times or lack of flow values, reflecting the gap in long-term monitoring. A streamflow record extension method called the Maintenance of Variance-Extension type 3 (MOVE.3) (Vogel and Stedinger 1985) was applied to estimate missing flow values or to extend the record at a short-record station based on daily streamflow values recorded at nearby, hydrologically similar index stations. On this basis, the FORTRAN Load Estimator (LOADEST) was used to estimate SS loads.

According to the lowest Akaike information criterion (AIC) values, some of the regression equations did not contain all terms (Sakamoto et al. 1986). The long-term average annual load of 31 stations was then standardized to the 2006 base year. The 2006 base year was chosen to be consistent with the latest explanatory geospatial data. Figure 7.4 shows the observed water flows (m^3/s) and the observed SS concentration (mg/l) at 31 monitoring stations in the Ishikari River Basin.

7.4.2.3 Sediment Source Data

Suspended sediment sources can be divided into sediments in highland areas, sediments in urban areas, and sediment erosion in river corridors (Langland et al. 2003). It is generally believed that the effects of land use lead to increased sediment loading and are therefore unintended consequences of human activities. In addition, land

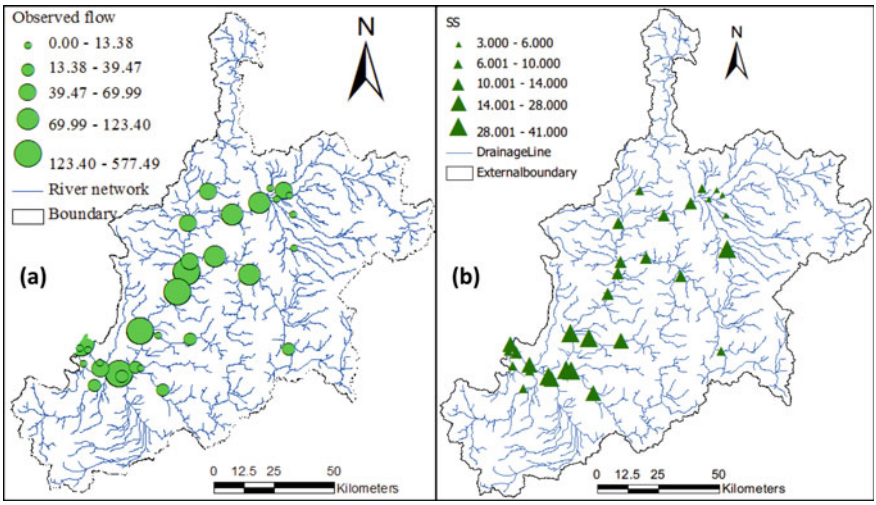

Fig. 7.4 Schematic showing **a** the observed water flows (m^3/s) and **b** the observed SS concentration (mg/l) at 31 monitoring stations

use and land-use change are also important factors affecting erosion and sediment yield. For example, when large areas of roads, roofs, and parking lots are covered with impervious surfaces, urbanization may eventually lead to a reduction in local surface erosion rates (Wolman 1967). The soil surface is increased due to the removal of natural plant cover, and agricultural land can greatly accelerate the erosion rate (Lal 2001). In addition, stream channel erosion may be the main source of sediment production in urbanized areas (Trimble 1997).

The SS source variables tested in the Ishikari SPARROW model include estimates of development sites, forest land, agricultural land, and river channels. Figure 7.5a shows 11 types of original land use in Ishikari River Basin, which were developed using data derived from the Policy Bureau of the Ministry of Land, Infrastructure, Transport and Tourism, Japan, 2006. They were then combined into four types (see Fig. 7.5b): developing land, forest land, agricultural land, and water land. Finally, different lands are allocated to individual sub-catchments to obtain the proportion for each land use using GIS zonal processes.

7.4.2.4 Environmental Setting Data

Climatic and landscape characteristics can affect SS transportation, which mainly contain climate, topography, and soil (Asselman et al. 2003; Dedkov and Mozzherin 1992). In this chapter, temperature, precipitation, slope, and soil permeability are used to assess the impact of "land-to-water" transport conditions. Mean annual temperature and precipitation data, representing the 20-year (1990–2010) average, were downloaded from the Japan Meteorological Agency. The results of them are

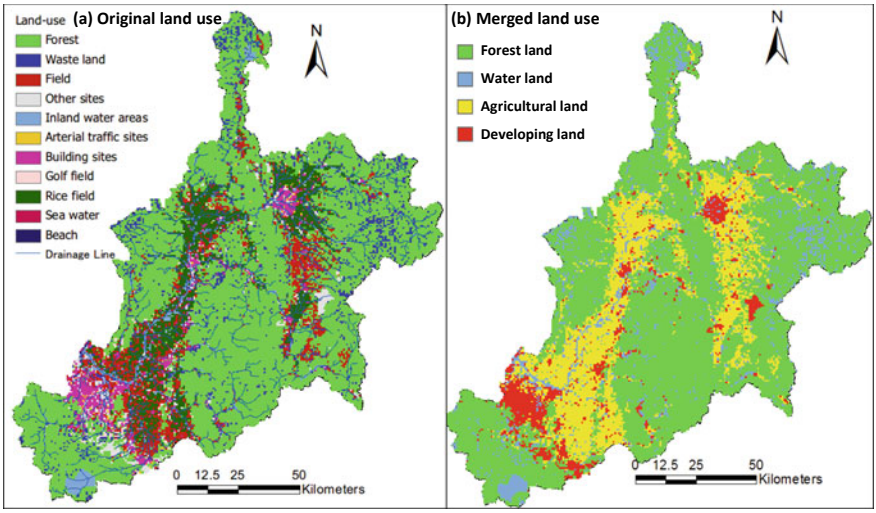

Fig. 7.5 Original and merged land use of the Ishikari River Basin, 2006

shown in Fig. 7.6a, b, which indicate that temperature ranged from 4.69 to 8.69 °C, and precipitation ranged from 1573.05 to 3013.57 mm. Figure 7.6c shows the slope of the basin, which is calculated using the GIS surface tool. Figure 7.6d shows the soil permeability and clay content, which are estimated using the data derived from the 1:5.000.000-scale FAO/UNESCO Soil Map of the World (Fao 1988) and the National and Regional Planning Bureau, Japan.

Loss of reaches and reservoirs are used as the mediating factors to influence the transfer of sediment from the river network. Reach-loss variable is nonzero only for stream reaches, and is defined for two separate categories including shallow-flowing (small) streams and deep-flowing (large) streams. Since the depth of the water flow is unknown, it is assumed that the water flow with a drainage area of less than 200 km^2 is a shallow and small streams. The loss of the reservoir is expressed in terms of the areal hydraulic load of the reservoir, which is calculated from the quotient of the average annual water storage outflow and surface area (Hoos and McMahon 2009).

7.5 Results

7.5.1 Streamflow Extension

Based on the MOVE.3 method and nearby long-time gauged stations, these stations with short recording records or missing flow values were filled and extended. Several criteria were used when selecting the long-term index stations (Nielsen 1999).

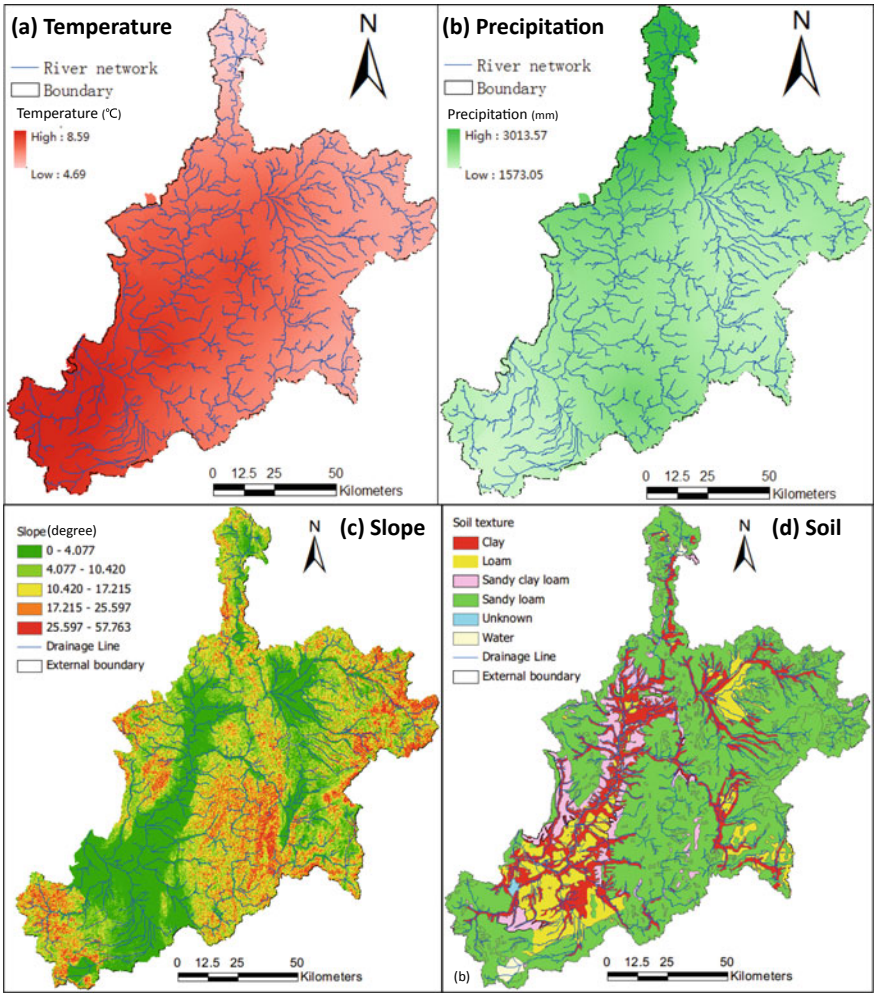

Fig. 7.6 Schematic showing the **a** temperature (°C), **b** precipitation (mm), **c** slope (degree), and **d** soil texture in Ishikari River Basin

Figure 7.7 shows Pearson's correlation coefficient (ρ), ranging from 0.79 (Umaoyi-bashi) to 0.96 (Yiwamizawa-oohashi), with an average value of 0.88, which suggests that relationship between the index stations and the studied stations were strong. The scatterplots of simultaneous average daily loads between the study stations and nearby index stations are shown in Fig. 7.8, indicating Yiwamizawa-oohashi station which had the best performance (see Fig. 7.8e).

After determining the index stations, the MOVE.3 method was used to extend the daily discharge records for each study station. During this process, two statistics including the root mean square error (RMSE) and the Nash–Sutcliffe efficiency

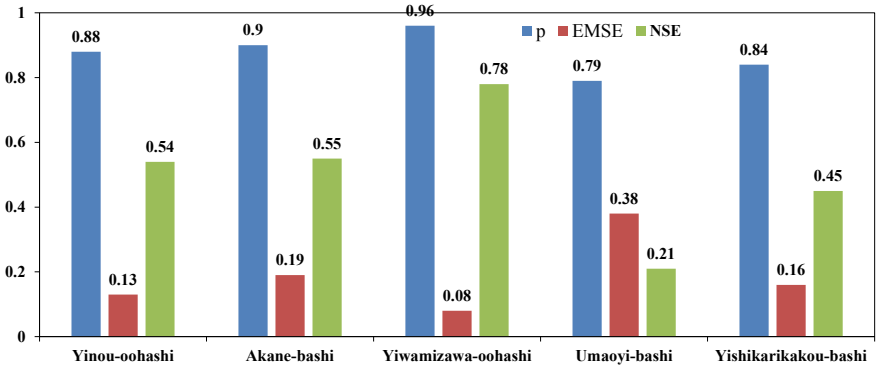

Fig. 7.7 Results of Pearson's correlation coefficient ρ for correlation between logarithms of river discharges at study stations and nearby index stations, RMSE of the estimating equations at each index station, and NSE of the model performance in river discharge simulations

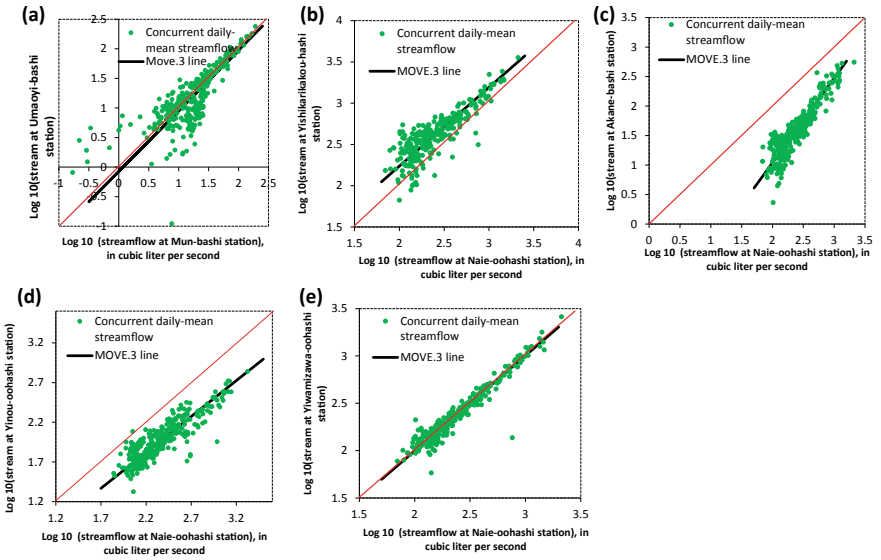

Fig. 7.8 The scatterplots of concurrent daily mean discharge between study stations and nearby index stations. The red line is the 1:1 line

(NSE, Legates, and McCabe 1999) were employed to evaluate the accuracy of the MOVE.3 method. The results were shown in Fig. 7.2. The RMSE ranged from 0.08 (Yiwamizawa-oohashi) to 0.38 (Umaoyi-bashi) and the NSE coefficient ranged from 0.21 (Umaoyi-bashi) to 0.78 (Yiwamizawa-oohashi), with an average of 0.51. Of them, Umaoyi-bashi had the largest RMSE and the smallest NSE, suggesting that the model performance of the site was relatively poor.

7.5.2 Regression Evaluation

Table 7.2 shows the regression coefficients, coefficients of determination (R^2), and AIC for load models used to estimate TN, TP, and SS at five sites in the Ishikari River Basin, Japan, 2000–2010. As can be seen in the figure, R^2 ranged from 71.86 to 90.94%, which indicates that the best-fit regression models for loads of TN, TP, and SS for the five studied sites performed well. Of them, Akane-bashi station was the best.

Meanwhile, the lowest AIC was the criterion to determine the best model and the AMLE was used to calculate the coefficients. For TN estimation at site Akane-bashi, the lowest of AIC was 0.729 and the coefficients a, b, c, d, e, f, and g were 7.694, 1.015, −0.066, 0.234, −0.040, and −0.017; while at site Umaoyi-bashi, the lowest of AIC was 0.928 and the coefficients employed were a (6. 354), b (0. 986), and c (0. 021). For TP estimation at site Akane-bashi, the lowest of AIC was 1.359 and the coefficients a, b, c, d, e, f, and g were 5.285, 1.064, −0.015, 0.044, −0.566, −0.024, and −0.002; while at site Yiwamizawa-oohashi, the lowest of AIC was 0.972 and the coefficients employed were a (7.445), b (1.286), c (0.095), d (−0.195), and e (−0.014). For SS estimation at site Akane-bashi, the lowest of AIC was 2.247 and the coefficients a, b, c, d, e, f, and g were 11.305, 1.597, 0.012, −0.051, −0.390, −0.040, −0.003, and 84.50; while at site Umaoyi-bashi, the lowest of AIC was 2.432 and the coefficients employed were a (10.103), b (1.592), c (0.138), d (0.363), e (0.348), f (−0.026), and g (−0.002).

7.5.3 Estimated Loads

This study mainly discussed the monthly, seasonal, and annual load estimates. For the sake of brevity, only estimated monthly average and measured instantaneous loads (kg/day) of TN, TP, and SS at site Akanebashi, 1985–2010, are displayed in time-series graphs (Fig. 7.9). As a measure of error associated with monthly average load estimates, the upper and lower 95% confidence intervals are also presented in Fig. 7.9. Yishikarikakou-bashi had the largest estimates, with TN, TP, and SS loads ranging from 8519.00 to 200189.00 kg/day (April 1999), 395.87 to 52299.00 kg/day (April 1999), and 92111.00–92500000.00 kg/day (September 2001), respectively. At all sites, monthly average TN, TP, and SS loads displayed seasonal fluctuations in both loads and in discharge from 1985 to 2010, even though the dates of peak discharge were not the same every year.

Figure 7.10 shows the estimated average loads of TN, TP, and SS for all stations from 1985 to 2010, which are averaged by the monthly averages for each month of the year (for example, the monthly average for all January, the average of February, the average of March, and so on). As can be seen from Fig. 7.10, April had the largest estimated average loads for TN, TP, and SS for all stations, the values of which are been in shown Fig. 7.6. After April, the estimated average load

Table 7.2 Regression coefficients, coefficients of determination (R^2), and AIC for load models used to estimate TN, TP, and SS at five sites in the Ishikari River Basin, Japan, 2000–2010

Water quality	Station's name	Regression coefficient							R^2 (%)	AIC
		a	b	c	d	e	f	g		
TN	Akane-bashi	7.694	1.015	−0.066	0.234	−0.040	−0.017		90.32	0.729
	Yinou-oohashi	9.061	0.973	0.017	0.178	0.185	−0.012	0.001	83.39	0.096
	Yiwamizawa-oohashi	10.144	0.932	0.149	0.125				90.92	−0.405
	Yishikarikakou-bashi	10.718	0.862	−0.074	−0.150	0.104	−0.011	0.001	81.61	0.123
	Umaoyi-bashi	6.354	0.986	0.021					89.22	0.928
TP	Akane-bashi	5.285	1.064	−0.015	0.044	−0.566	−0.024	−0.002	87.67	1.359
	Yinou-oohashi	6.039	0.963	0.103	0.185	−0.086	−0.014		71.86	1.078
	Yiwamizawa-oohashi	7.445	1.286	0.095	−0.004	−0.195	−0.014		85.29	0.972
	Yishikarikakou-bashi	7.886	1.164	0.101	0.150	0.031	−0.008	0.001	88.71	0.368
	Umaoyi-bashi	3.751	1.246	0.069	0.175	0.385	−0.017	−0.002	90.94	1.339
SS	Akane-bashi	11.305	1.597	0.012	−0.051	−0.390	−0.040	−0.003	84.50	2.247
	Yinou-oohashi	11.807	1.522	0.321	0.121	−0.117	−0.011	−0.003	75.68	1.777
	Yiwamizawa-oohashi	13.641	1.972	0.100	−0.124	−0.209	−0.029	−0.002	85.98	1.752
	Yishikarikakou-bashi	13.283	2.089	0.305	0.223	−0.141	−0.033		85.58	1.815
	Umaoyi-bashi	10.103	1.592	0.138	0.363	0.348	−0.026	−0.002	84.21	2.432

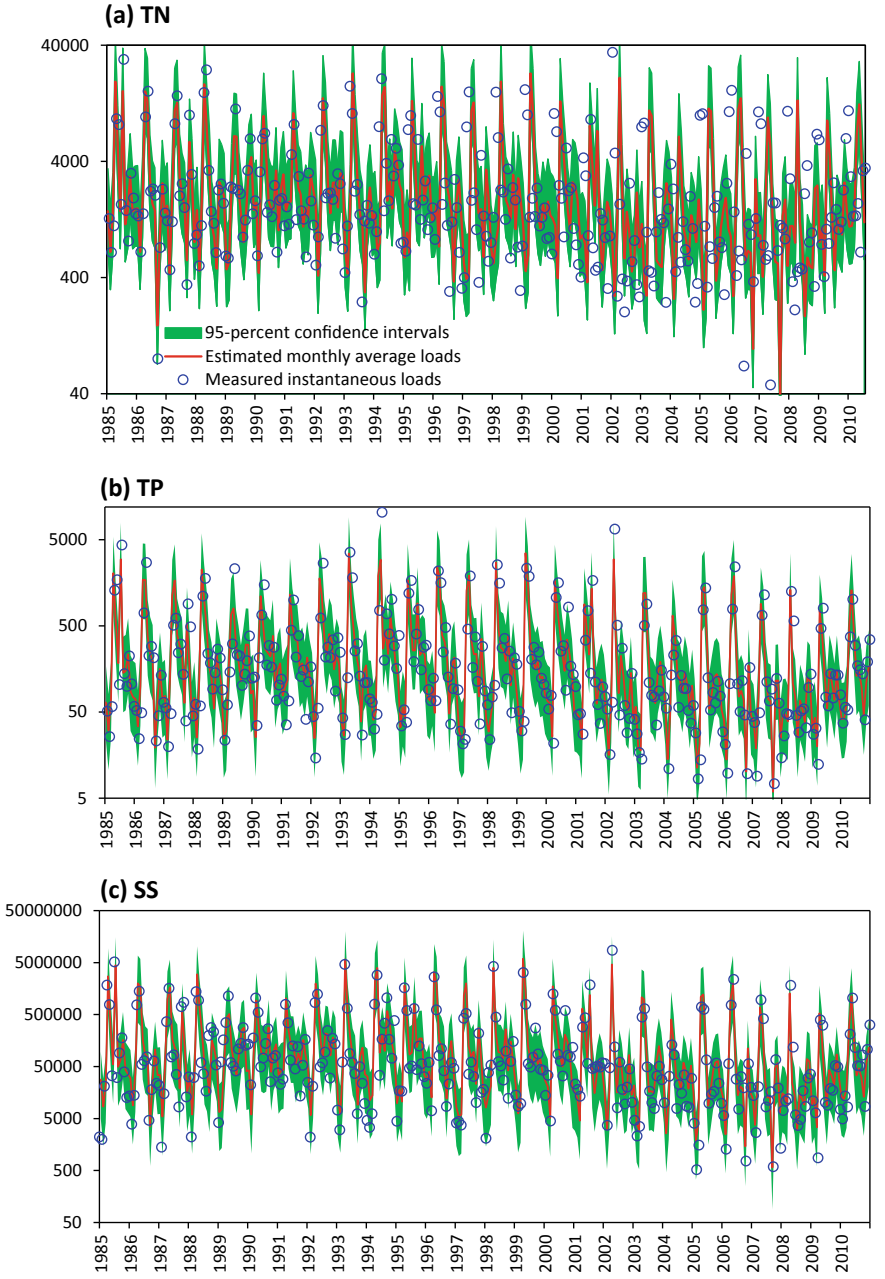

Fig. 7.9 Estimated monthly average and measured instantaneous loads (kg/day) of TN, TP, and SS at site Akanebashi, 1985–2010

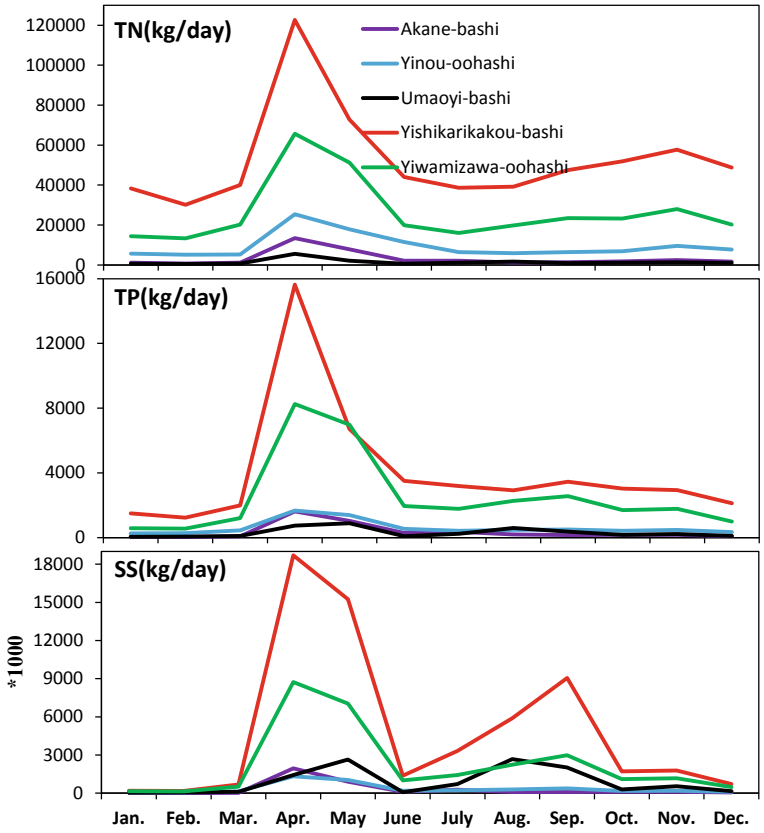

Fig. 7.10 Estimated monthly loads of TN, TP, and SS at five sites on the Ishikari River, from the January 1985 to the December 2010

drops and then increases. Typically, TP and SS peak in September, while loads in January, February, and March were relatively low. At Yishikarikakou-bashi, the values of TN, TP, and SS estimates were 122629.31 kg/day, 15630.62 kg/day, and 18694484.69 kg/day, respectively; at Yiwamizawa-bashi, the values of TN, TP, and SS estimates were 65651.08 kg/day, 8259.08 kg/day, and 8741123 kg/day, respectively; and at Yinou-bashi, the values of TN, TP, and SS estimates were 25375.77 kg/day, 1668.73 kg/day, and 1321272 kg/day, respectively.

Estimated seasonal loads of TN, TP, and SS at five sites were highly variable between 1985 and 2010 in the Ishikari River and its tributaries, with the greatest loads occurring in the spring and the smallest loads occurring in the winter (Fig. 7.10), reflecting fluctuations in discharge as a result of the combined effects of seasonal runoff patterns, the exact timing of which vary from year to year. At site Akane-bashi, TN load decreased from 8146.00 kg/day in spring to 1191.00 kg/day in winter, TP load decreased from 907.00 to 60.30 kg/day, and

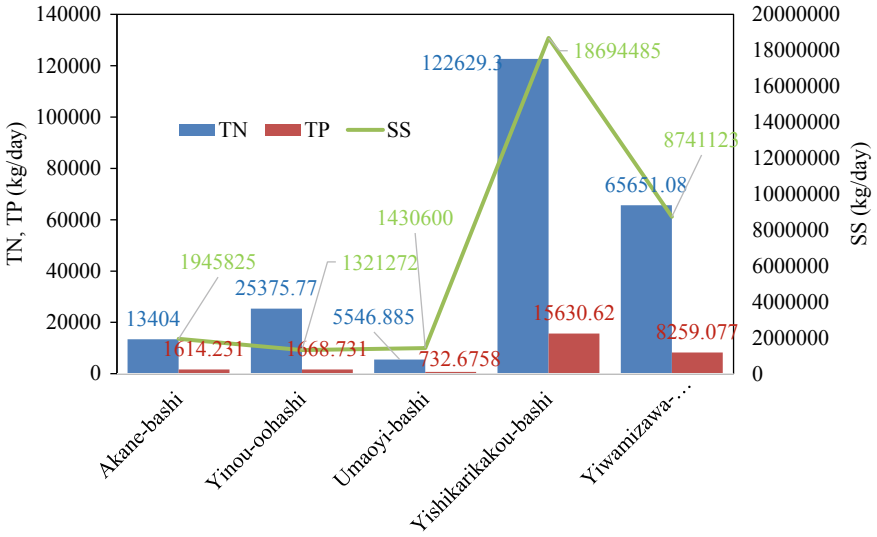

Fig. 7.11 Estimated average loads of TN, TP, and SS in April, at five sites on the Ishikari River, January 1985 through December 2010 (kg/day)

SS decreased from 956854.00 to 26906.00 kg/day. At site Yishikarikakou-bashi, TN load decreased from 78478.00 kg/day in spring to 39091.00 kg/day in winter, TP load decreased from 8110.00 to 1619.00 kg/day, and SS decreased from 11470000.00 to 367458.00 kg/day. Seasonal fluctuations were consistent with monthly fluctuations (Fig. 7.10). Regardless of season, site Yishikarikakou-bashi had the largest loads of TN, TP, and SS, far more than at other sites, the seasonal mean of which were 46 702, 3 560, and 1 991 033 kg/day (Fig. 7.11).

Between 1985 and 2010, the estimated seasonal load of TN, TP, and SS at the five locations of the Ishikari River and its tributaries varied greatly, with the largest loads in spring and the least load in winter (Fig. 7.12), which were line with the seasonal runoff patterns of every year. At the Akane-bashi station, the total nitrogen load decreased from 8146.00 kg/day in spring to 1191.00 kg/day in winter, and the total phosphorus load decreased from 907.00 to 60.30 kg/day, while SS decreased from 956854.00 to 26906.00 kg/day. At the Yishikarikakou-bashi site, the TN load decreased from 78478.00 kg/day in spring to 39091.00 kg/day in winter, the TP load decreased from 8110.00 to 1619.00 kg/day, and the SS decreased from 11470000.00 to 367458.00 kg/day. At the Yiwamizawa-bashi site, the TN load decreased from 45481.00 kg/day in spring to 16067.00 kg/day in winter, the TP load decreased from 5449.00 to 712.86 kg/day, and the SS decreased from 5392.07 to 256.53 kg/day.

Seasonal fluctuations are consistent with monthly fluctuations. As can be seen in Fig. 7.13, the Yishikarikakou-bashi site had the highest seasonal TN, TP, and SS loads, far exceeding other sites, with seasonal averages of 46,702, 3,560, and 1,991,033 kg/day, followed by Yiwamizawa-oohashi site (TN(26233.50 kg/day), TP(2553.00 kg/day), and SS(2250293.00 kg/day)).

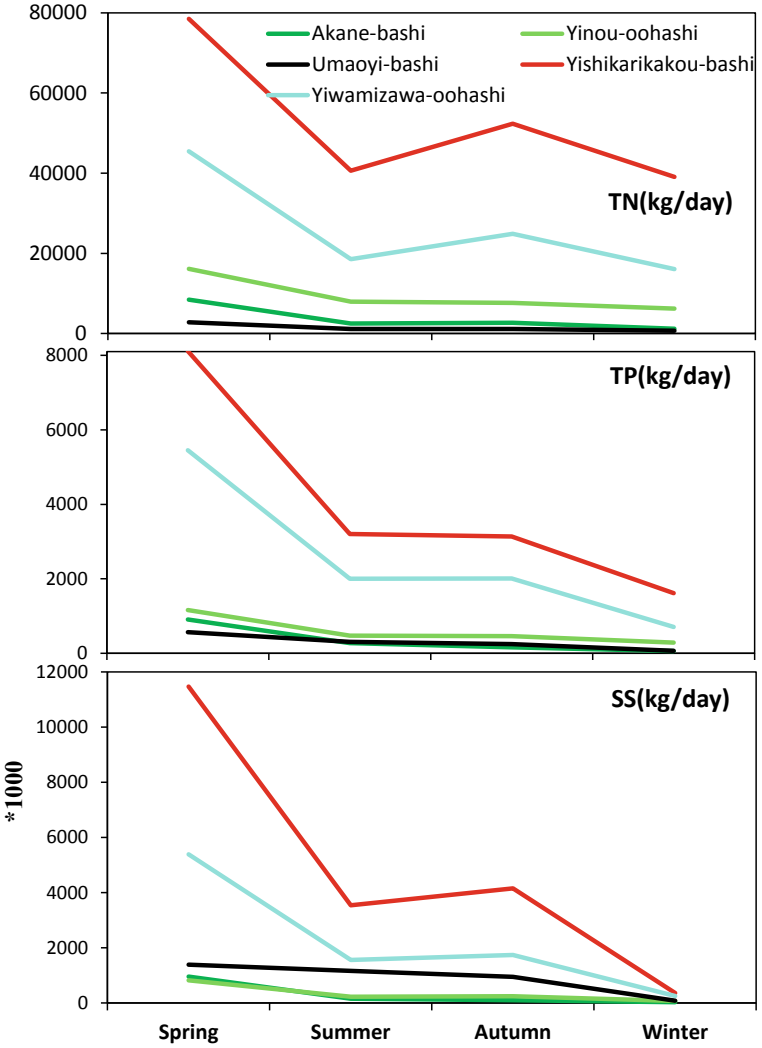

Fig. 7.12 Estimated seasonal average loads of TN, TP, and SS at five sites on the Ishikari River, January 1985 through December 2010

7.5.4 Trends of the Estimated Yearly Loads of TN, TP, and SS

Since the Yishikarikakou-bashi site is located on the inlet of the Ishikari River, this study calculated the trends of the estimated yearly loads of TN, TP, and SS at this station, which could reflect changes of water quality for the whole Ishikari River Basin. The results are shown in Fig. 7.14, which suggest that a significant decreasing trend was detected for all the water quality indices at Yishikarikakou-bashi site

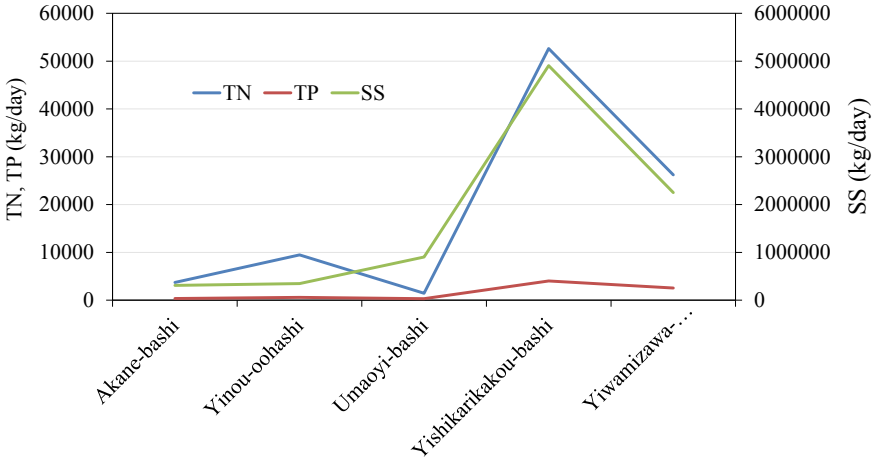

Fig. 7.13 Estimated seasonal loads of TN, TP, and SS at five sites on the Ishikari River (kg/day)

from 1985 to 2010. The Mann–Kendall Z values of TN, TP, and SS were −3.79, −2.42, and −2.82, respectively, and the decrease of TN, TP, and SS was about 635.04 kg/day, 65.68 kg/day, and 217257 kg/day for each year, respectively. Results show a significant improvement in water quality in Ishikari River Basin.

7.5.5 Results of SPARROW SS Model

7.5.5.1 Model Calibration

After parameter adjustment, we successfully established the final SPARROW suspended sediment model for the Ishikari River Basin, which contains four source variables (agricultural land, forest land, developing land, and streambed (stream channels)), three landscape transport variables (precipitation, slope, and soil permeability), two in-stream loss coefficients (small stream (drainage area $\leq 200\ \text{km}^2$) and large stream (drainage area $> 200\ \text{km}^2$)), as well as reservoir attenuation describing removal/deposition in reservoirs (see Tables 7.1 and 7.3). Table 7.3 lists the model calibration results for the logarithmic transformation and the nonlinear least-squares estimation of the sum in Eq. (7.11), which explains about 95.96% (R^2) of the spatial variation in the natural logarithm of the average annual suspended sediments in the Ishikari River Basin. The mean square error (MSE) of 0.323 indicates that the SS predicted by the model matches the observed load very well. For comparison, the accuracy of the results is worse than other SPARROW models such as Waikato SPARROW model ($R^2 = 0.97$ and MSE = 0.14, calibrated using 37 stations) due to different parameters and the accuracy of calibration data (Alexander et al. 2002).

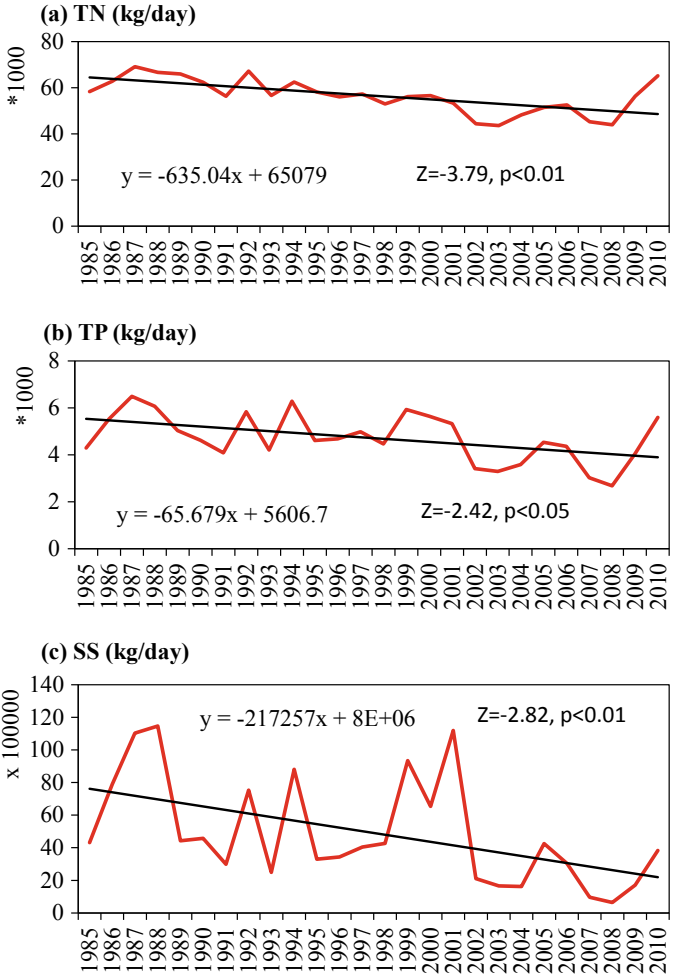

Fig. 7.14 Trends of estimated yearly loads of TN, TP, and SS at Yishikarikakou-bashi site on the Ishikari River (kg/day)

Figure 7.15a shows the observed and predicted SS flux (kg/year) at 31 monitoring sites included in the Ishikari SPARROW model (Natural logarithm transformation applied to observed and predicted values). As we can see from the figure, the fitting line is close to the red dashed line (1:1 line), suggesting that the predicted values were close to the observed values. Figure 7.15b shows the model residuals for 31 monitoring stations used to calibrate the final Ishikari SPARROW model which reveals that high-predicted (<0) monitoring sites mainly exist in the central part of the Ishikari River Basin, and high-predicted (>0) monitoring sites exist in the upper and lower river. Schwarz et al. 2006 argued that standardized residual greater than

Table 7.3 SPARROW estimates of model statistics for Ishikari River Basin SS based on the 31 monitoring stations

Model parameters	Coefficient units	Estimated coefficient	Standard error	P-value
SS sources				
Developing land	kg/km^2/year	1006.267	508.503	0.028
Forest land	kg/km^2/year	75.554	31.058	0.011
Agricultural land	kg/km^2/year	234.211	121.7511	0.036
Streambed (stream channels)	kg/km/year	123.327	99.567	0.113
Land-to-water loss coefficient				
Slope	–	0.349	0.094	<0.001
Soil permeability	h/cm	−9.195	2.431	<0.001
Precipitation	mm	0.007	0.002	<0.002
In-stream loss rate				
Small stream (drainage area ≤200 km^2)	day^{-1}	−0.044	0.011	<0.001
Big stream (drainage area >200 km^2)	day^{-1}	0.000012	0.0068	>0.050
Reservoir-loss	m/year	26.283	4.364	<0.001
Model diagnostics				
Mean square error	0.323			
Number of observations	31			
R-squared	0.9596			

Notes This table indicates the overall model calibration results, statistical parameter estimates, standard errors, and probability levels for modeled explanatory sediments variables. All sources and storage items are subject to non-negative estimates for more realistic physical simulation of the suspended sediment transport. Due to this specification, the statistical significance of the source and aquatic storage coefficient estimates is evaluated as a one-sided p statistic, and the two-sided values are used to assess the probability levels for land-to-water parameters (Schwarz et al. 2006)

3.6 are generally considered outliers and require further investigation. Therefore, the final model did not show evidence of large prediction bias at the monitoring site.

All simulated source variables were statistically significant ($P < 0.05$) except for the river channel and indicated the average level of sediment supply (Table 7.3). The developing land produced the largest intrinsic sediments, with an estimated value of approximately 1006.267 kg/km^2/year, which is line with the results from Brakebill et al. (2010) and Schwarz (2008). The sediment yield of agricultural land is the second highest, with an estimated value of about 234.211 kg/km^2/year, while the sediment yield of forest land is the lowest, with an estimated value of about 75.554 kg/km^2/year.

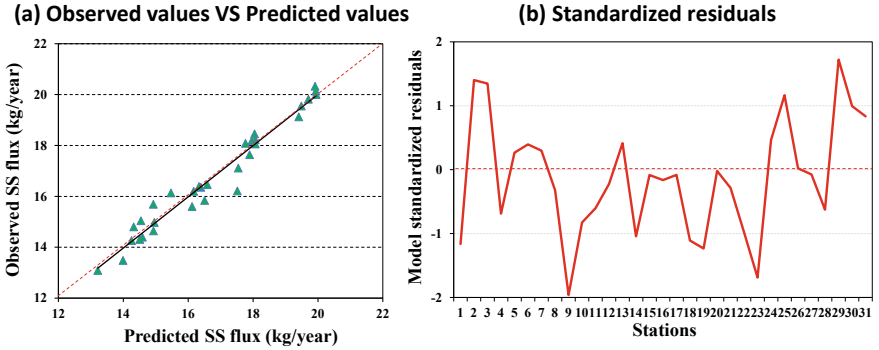

Fig. 7.15 **a** Observed and predicted SS flux (kg/year) at 31 monitoring sites included in the Ishikari SPARROW model (Natural logarithm transformation applied to observed and predicted values); **b** Model residuals for 31 monitoring stations used to calibrate the final Ishikari SPARROW model

Land-to-water delivery for sediment land sources is powerfully mediated by watershed slope, soil permeability, and rainfall, all of which are statistically significant (Table 7.3). As expected, Table 7.3 shows that sediment produced from land transport to rivers is most efficient in areas with greater basin slope, less permeable soils, and greater rainfall, which is consistent with the results calculated by Brakebill et al. (2010). The alteration of these factors can directly and indirectly cause changes in sediment degradation and deposition, and, finally, to the sediment yield (Luce and Black 1999; Nelson and Booth 2002). Increased rainfall amounts and intensities can directly increase surface runoff, leading to greater rates of soil erosion (Nearing et al. 2005; Ran et al. 2012) with consequences for productivity of farmland (Julien and Simons 1985). Watershed slope and soil permeability have a powerful influence on potential surface runoff as they affect the magnitude and rate of eroded sediment that may be transported to streams (Brakebill et al. 2010).

The slope of the watershed, soil permeability, and precipitation have an important impact on the suspended sediment transport from land to water. Table 7.3 shows that suspended sediments produced from land transport to rivers are most effective in regions with larger watershed slopes, less permeable soils, and greater precipitation, which is consistent with the calculations of Brakebill et al. (2010). Changes in these factors can directly and indirectly lead to changes in sediment degradation and sedimentation, and ultimately to changes in suspended sediments yield (Luce and Black 1999; Nelson and Booth 2002). For example, increased precipitation amounts and intensities can directly increase surface runoff, which can bring greater soil erosion rates (Nearing et al. 2005; Ran et al. 2012), affecting farmland productivity (Julien and Simons 1985).

Table 7.3 also shows that the estimated coefficient for large streams and small streams is about 0.000012 day^{-1} and -0.044 day^{-1}, respectively, which suggests that suspended sediments are removed from large streams and accumulated in small streams. These results are not in line with one previous point that the river channels with high flow can increase the amount of sediments generated from stream channels

(Schwarz 2008). In the reservoir, sediment storage was statistically significant and estimated to be approximately 26.283 m/year, which is similar to the result of the conterminous U.S. SPARROW model (36 m/year) (Schwarz 2008).

7.5.5.2 Model Application

Figure 7.16a shows the spatial distribution of total suspended sediments yields, ranging from 0.034 to 1190 kg/ha/year (mean = 101 kg/ha/year). The distribution also shows the total suspended sediments yields concentrated in the secondary watershed in the middle and lower reaches of the Shishou River, which suggests that the sediments yields relate to the river network. Figure 7.16b shows the spatial distribution of increased suspended sediments yields, which indicates that much of the incremental sediment yields are distributed in regions with high total suspended sediments yields. The largest value of the increased suspended sediments yields is greater than 150 kg/ha/year.

Figure 7.16 also illustrates the percentage of total incremental flux produced by (c) agricultural lands, (d) developing lands, (e) forested lands, and (f) stream channels, indicating the relative contribution of various sources to each sub-basin. As shown in the figure, the proportion of agricultural-land sediment yields was greater than 50%, in many sub-basins with high total sediment yields. The same distribution was found in the proportion of predicted forest-land sediment yield and predicted steam channels yield, and all these two sources produced low suspended sediments in the Ishikari River Basin. Figure 7.17 shows the total incremental flux generated for agricultural lands, developing lands, forested lands, and stream channels. As shown in the figure, agricultural lands produced the largest suspended sediments, up to 35.11%, followed by forested lands (23.42%), developing lands (22.91%), and stream channels (18.56%).

7.6 Discussions

7.6.1 Large Loads of TN, TP, and SS at Site Yishikarikakou-bashi

The Yishikarikakou-bashi site had the highest loads of TN, TP, and SS in both monthly and seasonal loads. The reason is that this site is located in the lower reaches of the Ishikari River and has the highest average discharge, which is the primary driver of constituent delivery to coastal waters (Fig. 7.18). Constituents from the upper, middle, and lower reaches of the mainstream and the Uryū and Yūbari Tributaries move together and are discharged at the Yishikarikakou-bashi Site.

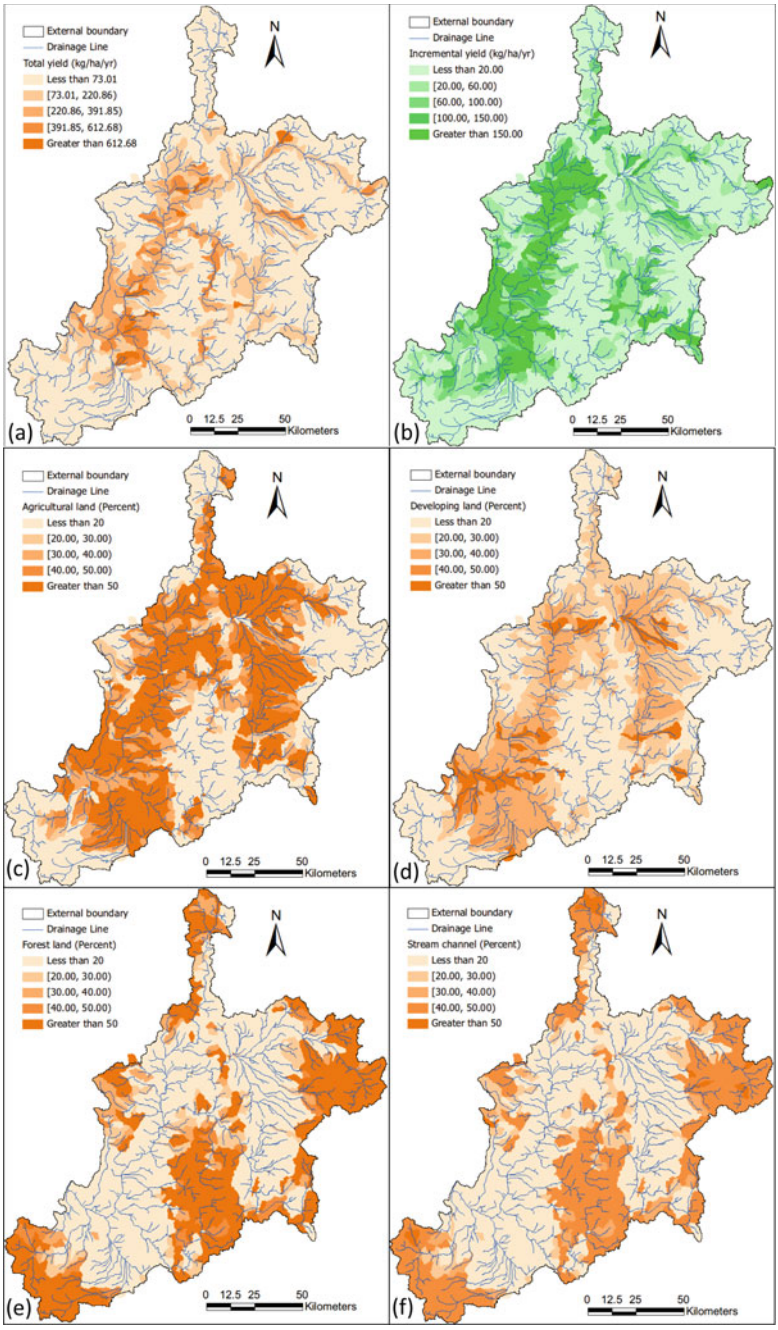

Fig. 7.16 Map showing the spatial distribution of **a** total suspended sediment yields, **b** incremental suspended sediment yields, **c** sediments produced by agricultural lands, **d** sediments produced by developing lands, **e** sediments produced by forest lands, and **f** sediments produced by stream channels

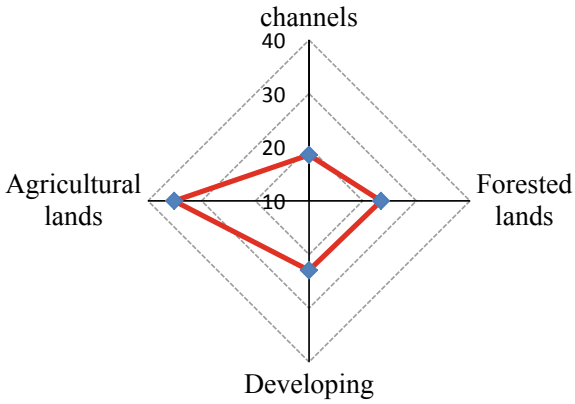

Fig. 7.17 The total incremental flux generated for agricultural lands, developing lands, forested lands, and stream channels

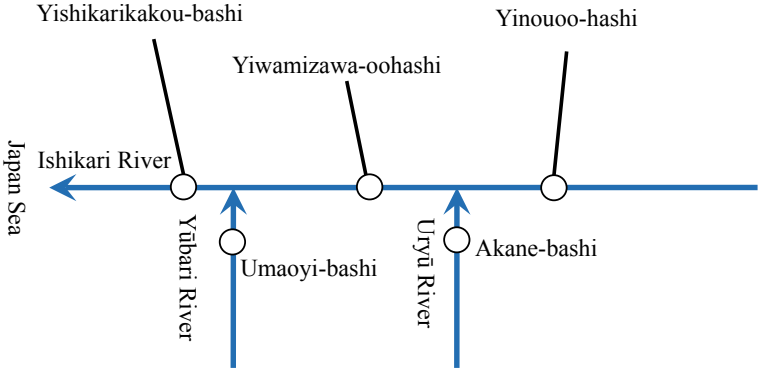

Fig. 7.18 Schematic diagram of the Ishikari River and five studied sites

7.6.2 Decreasing Trends of TN, TP, and SS Loads

From Fig. 7.9, we can see a downward trend of TN, TP, and SS load (most obvious was the decline of SS after 2001), which is in line with the result from Luo et al. (2011). Many researchers have shown that land use has a large impact on water quality and there is a significant correlation between water quality parameters and land-use types (Tu 2011; Woli et al. 2004). In Hokkaido, the urbanization process was accelerating, leading to an increase in the population of the Ishikari River Basin. Table 7.4 shows that the population of the Ishikari River Basin has increased from 760132 in 1920 to 3124348 in 2005, with 32.2% of Hokkaido's population in 1920 to 55.5% of Hokkaido's population in 2005. Urbanization has increased the pressure on the Ishikari River Basin, such as the increase of flooding, river erosion, and so on (Klein 2007).

However, numerous water management measures have been implemented in Japan to prevent deterioration of water quality. First of all, many polices and laws have been

Table 7.4 Increasing trend of people that live in the Ishikari River Basin from 1920 to 2005

Year	Hokkaido	Ishikari river Basin	Percentage (%)
1920	1599051	760132	32.2
1955	2942693	1830394	38.3
1965	3044706	2127094	41.4
1985	2876589	2802850	49.4
2005	2507785	3124348	55.5

enacted to reduce and mitigate pollution, especially since 2000 (see Fig. 7.19), leading to a comprehensive policy framework concerning water pollution control. In the 1990s, "Basic Environment Law" was enacted to set environmental quality standards for water quality. "Drinking Water Sources Law", "Laws Concerning Special Measures for Conservation of Drinking Water Sources", and "Law on Livestock Excreta Management and Recycling" were enacted to keep water sources from being polluted. In the 2000s, "Law Concerning Special Measures against Dioxins" and "Soil Contamination Countermeasures Law" were enacted to prevent pollution caused by hazardous substances. Some important international conventions concerning the prevention of water pollution including the "Convention on the Prevention and of Marine Pollution by Dumping of Wastes and other Matter", "International Convention for the Prevention of Pollution from Ships", and "International Convention for the Control and Management of Ships' Ballast and Sediments" were also enforced to protect water quality.

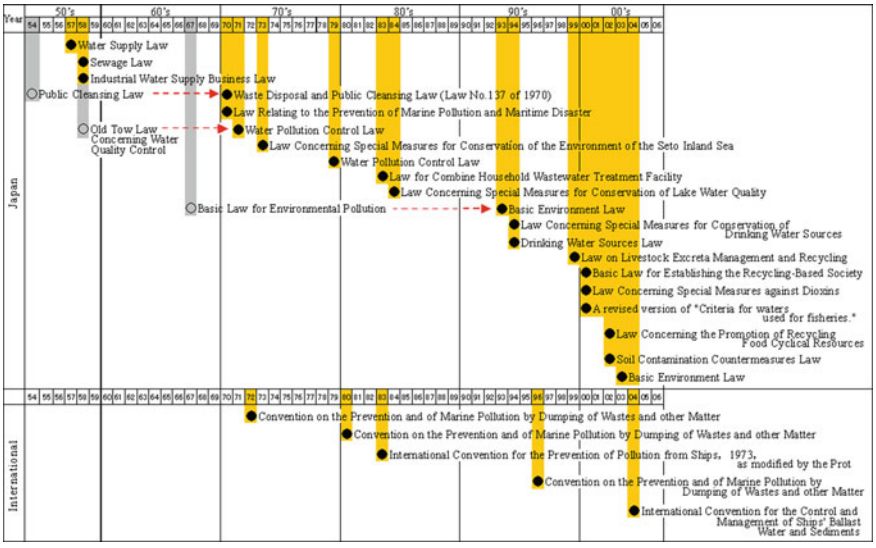

Fig. 7.19 A History of enactment of laws concerning water pollution control (*Source* https://www.jetro.go.jp/ttppoas/special/env_rep_english/env_rep_03_1.html)

However, Japan has taken many water management measures to prevent water quality deterioration. First, especially since 2000, many policies and laws to reduce and mitigate pollution have been enacted (see Fig. 7.19), resulting in a comprehensive policy framework for water pollution control. In the 1990s, the "Basic Environment Law" was enacted to set environmental quality standards for water quality for whole Japan. "Drinking Water Sources Law", "Laws Concerning Special Measures for Conservation of Drinking Water Sources", and "Law on Livestock Excreta Management and Recycling" were promulgated to prevent pollution of water sources. In the 2000s, the "Law Concerning Special Measures against Dioxins" and "Soil Contamination Countermeasures Law" were promulgated to prevent pollution caused by harmful substances. Some important international conventions on the prevention of water pollution were also implemented.

In addition, with the urbanization of Japan, the water infrastructure including the sewer system has also expanded. As shown in Table 7.5, the length, processing area, processing capacity, and coverage of the sewer system in Sapporo City had increased from 910.30 km, 1771 ha, 115.4 $\times$ 10^3 m^3/day, and 19.20% in 1970 increased to 8139.70 km, 24611 ha, 1173.80 $\times$ 10^3 m^3/day, and 99.70% in 2009, respectively. Meanwhile, improvements in industrial water treatment and wastewater treatment systems and improvements in "Jukasou" (Japan's domestic wastewater treatment system) had also helped to reduce wastewater flow (Luo et al. 2011). Overall, improvements in policies and laws and improvements in water infrastructure in recent years have led to a downward trend in TN, TP, and SS loads.

Table 7.5 Changes of length of sewer system, processing area, processing capacity, and coverage rate in Sapporo (Data from https://www.city.sapporo.jp/kurashi/suido_gesui/index.html)

Year	Length of sewer system (km)	Processing area (ha)	Processing capacity (thousands of m^3/day)	Coverage rate of sewer system (%)
1970	910.30	1,771	115.4	19.20
1975	2,437.40	8,552	423	64.50
1980	4,170.30	14,638	729	85.90
1985	5,887.20	18,786	948.1	91.80
1990	6,753.70	20,602	986.8	95.40
1995	7,348.20	22,933	1,044.80	98.60
2000	7,713.70	23,813	1,089.80	99.20
2005	8,006.60	24,402	1,173.80	99.50
2009	8,139.70	24,611	1,173.80	99.70

7.7 Conclusions

In this chapter, we firstly estimated the total nitrogen (TN), total phosphorus (TP), and suspended sediment (SS) loads in Ishikari River Basin, from January 1985 to December 2010, and then successfully established the final SPARROW suspended sediment model for the Ishikari River basin, which contains four source variables (agricultural land, forest land, developing land, and streambed (stream channels)), three landscape transport variables (precipitation, slope, and soil permeability), two in-stream loss coefficients (small stream (drainage area $\leq 200\ km^2$) and large stream (drainage area $> 200\ km^2$)), as well as reservoir attenuation describing removal/deposition in reservoirs. The significant conclusions of the calibration procedure and model application are summarized below:

(1) The loads of TN, TP, and SS were largest in April, and spring, reflecting the fluctuation of seasonal runoff patterns in the Ishikari River Basin. Also, the Yishikarikakou-bashi site had the highest water quality loads due to which it is located in the lower reaches of the Ishikari River.
(2) A decreasing trend was found in TN, TP, and SS loads in Ishikari River Basin from 1985 to 2010, because of improvements in policies and laws and improvements in water infrastructure in recent years.
(3) The calibration results of SPARROW model account for approximately 95.96% of the spatial variation in the natural logarithm of mean annual SS flux (kg/year) and show relatively small prediction errors based on 31 monitoring stations.
(4) Developing land has the largest intrinsic sediment yield at around 1006.267 kg/km^2/year, followed by agricultural land (234.211 kg/km^2/year), stream channels (123.327 kg/km^2/year), and forest land (75.554 kg/km^2/year). Reservoir attenuation (26.283 m/year) is statistically significant, indicating that reservoirs can play an important role in sediment retention.
(5) The total sediment yield and incremental production are concentrated in the middle and lower reaches of the Ishikari River, indicating that these sub-basins are most susceptible to erosion. The percentages of total incremental fluxes from agricultural land, developing land, forest land, and river channels were 35.11%, 23.42%, 22.91%, and 18.56%, respectively.

References

Alexander, R. B., Elliott, A. H., Shankar, U., & McBride, G. B. (2002). Estimating the sources and transport of nutrients in the Waikato River Basin, New Zealand. *Water Resources Research, 38,* 1268.

Alexander, R. B., Smith, R. A., & Schwarz, G. E. (2000). Effect of stream channel size on the delivery of nitrogen to the Gulf of Mexico. *Nature, 403,* 758–761.

Alexander, R. B., Smith, R. A., Schwarz, G. E., Boyer, E. W., Nolan, J. V., & Brakebill, J. W. (2007). Differences in phosphorus and nitrogen delivery to the Gulf of Mexico from the Mississippi River Basin. *Environmental Science and Technology, 42,* 822–830.

Armour, J. D., Hateley, L. R., & Pitt, G. L. (2009). Catchment modelling of sediment, nitrogen and phosphorus nutrient loads with SedNet/ANNEX in the Tully–Murray basin. *Marine & Freshwater Research, 60,* 1091–1096.

Asahi, K., Kato, K., & Shimizu, Y. (2003). Estimation of sediment discharge taking into account tributaries to the Ishikari River. *Journal of Natural Disaster Science, 25,* 17–22.

Asselman, N. E. M., Middelkoop, H., & Van Dijk, P. M. (2003). The impact of changes in climate and land use on soil erosion, transport and deposition of suspended sediment in the River Rhine. *Hydrological Processes, 17,* 3225–3244.

Beasley, D. B., Huggins, L. F., & Monke, E. J. (1980). ANSWERS: A model for watershed planning. *Transactions of the ASAE, 23*.

Brakebill, J. W., Ator, S. W., & Schwarz, G. E. (2010). Sources of Suspended-Sediment flux in streams of the chesapeake bay watershed: A regional application of the SPARROW model1. *JAWRA Journal of the American Water Resources Association, 46,* 757–776.

Carpenter, S. R., Caraco, N. F., Correll, D. L., Howarth, R. W., Sharpley, A. N., & Smith, V. H. (1998). Nonpoint pollution of surface waters with phosphorus and nitrogen. *Ecological Applications, 8,* 559–568.

Christensen, V. G., Jian, X., Ziegler, A. C., & Demonstration, E. B. G. R. (2000). *Regression analysis and real-time water-quality monitoring to estimate constituent concentrations, loads, and yields in the Little Arkansas River, south-central Kansas, 1995–99*. US Department of the Interior, US Geological Survey.

Dedkov, A. P., & Mozzherin, V. I. (1992). Erosion and sediment yield in mountain regions of the world. In *Erosion, debris flows and environment in mountain regions*, no. 209 (pp. 29–36).

Duan, W., He, B., Sahu, N., Luo, P., Nover, D., Hu, M., et al. (2017). Spatiotemporal variability of Hokkaido's seasonal precipitation in recent decades and connection to water vapour flux. *International Journal of Climatology, 37,* 3660–3673.

Duan, W., Takara, K., He, B., Luo, P., Nover, D., & Yamashiki, Y. (2013). Spatial and temporal trends in estimates of nutrient and suspended sediment loads in the Ishikari River, Japan, 1985 to 2010. *Science of the Total Environment, 461,* 499–508.

Duan, W. L., He, B., Takara, K., Luo, P. P., Nover, D., & Hu, M. C. (2015). Modeling suspended sediment sources and transport in the Ishikari River basin, Japan, using SPARROW. *Hydrology and Earth System Sciences, 19*, 1295–1306.

Duan, W. L., He, B., Takara, K., Luo, P. P., & Yamashiki, Y. (2012). Estimating the sources and transport of nitrogen pollution in the Ishikari River Basin, Japan. In *Advanced materials research* (pp. 3007–3010).

FAO. (1988). Soil map of the world, FAO/Unesco/ISRIC. Retrieved May 2019, from http://www.fao.org/soils-portal/soil-survey/soil-maps-and-databases/faounesco-soil-map-of-the-world/en/.

Ferguson, R. I. (1986). River loads underestimated by rating curves. *Water Resources Research, 22,* 74–76.

Gilbert, R. O. (1987). *Statistical methods for environmental pollution monitoring*. New York, NY: Van Nostrand Reinhold.

Gruber, N., & Galloway, J. N. (2008). An Earth-system perspective of the global nitrogen cycle. *Nature, 451,* 293–296.

Helsel, D. R., & Hirsch, R. M. (1992). *Statistical methods in water resources*. Elsevier Science.

Hoos, A. B., & McMahon, G. (2009). Spatial analysis of instream nitrogen loads and factors controlling nitrogen delivery to streams in the southeastern United States using spatially referenced regression on watershed attributes (SPARROW) and regional classification frameworks. *Hydrological Processes, 23,* 2275–2294.

Ishida, T., Nakayama, K., Okada, T., Maruya, Y., Onishi, K., & Omori, M. (2010). Suspended sediment transport in a river basin estimated by chemical composition analysis. *Hydrological Research Letters, 4,* 55–59.

Jeon, J. H., Lim, K. J., Yoon, C. G., & Engel, B. A. (2011). Multiple segmented reaches per subwatershed modeling approach for improving HSPF-Paddy water quality simulation. *Paddy and Water Environment, 9,* 193–205.

Johanson, R. C., Imhoff, J. C., & Davis, H. H. (1980). *Users manual for hydrological simulation program-FORTRAN (HSPF)*. Environmental Research Laboratory, Office of Research and Development, US Environmental Protection Agency.

Johnes, P. J. (2007). Uncertainties in annual riverine phosphorus load estimation: Impact of load estimation methodology, sampling frequency, baseflow index and catchment population density. *Journal of Hydrology, 332,* 241–258.

Julien, P. Y., & Simons, D. B. (1985). Sediment transport capacity of overland flow. *Transactions of the ASAE, 28,* 755–762.

Kendall, M. G. (1975). *Rank correlation methods*. London: Charles Griffin.

Kirsch, K., Kirsch, A., & Arnold, J. G. (2002). *Predicting sediment and phosphorus loads in the Rock River basin using SWAT*. Forest 971, 10.

Klein, R. D. (2007). Urbanization and stream quality impairment1. *JAWRA Journal of the American Water Resources Association, 15,* 948–963.

Kulasova, A., Smith, P. J., Beven, K. J., Blazkova, S. D., & Hlavacek, J. (2012). A method of computing uncertain nitrogen and phosphorus loads in a small stream from an agricultural catchment using continuous monitoring data. *Journal of Hydrology, 458–459,* 1–8.

Lal, R. (2001). Soil degradation by erosion. *Land Degradation and Development, 12,* 519–539.

Langland, M. J., Cronin, T. M., & US, G. S. (2003). *A summary report of sediment processes in Chesapeake Bay and watershed*. US Department of the Interior, US Geological Survey.

Legates, D. R., & McCabe, G. J., Jr. (1999). Evaluating the use of "goodness-of-fit" measures in hydrologic and hydroclimatic model validation. *Water Resources Research, 35,* 233–241.

Li, S., Li, J., & Zhang, Q. (2011). Water quality assessment in the rivers along the water conveyance system of the Middle Route of the South to North Water Transfer Project (China) using multivariate statistical techniques and receptor modeling. *Journal of Hazardous Materials, 195,* 306–317.

Li, S., Liu, W., Gu, S., Cheng, X., Xu, Z., & Zhang, Q. (2009). Spatio-temporal dynamics of nutrients in the upper Han River basin, China. *Journal of Hazardous Materials, 162,* 1340–1346.

Liew, M. W. V., Feng, S., & Pathak, T. B. (2012). Climate change impacts on streamflow, water quality, and best management practices for the Shell and Logan Creek Watersheds in Nebraska, USA. *International Journal of Agricultural and Biological Engineering, 5,* 13–34.

Luce, C. H., & Black, T. A. (1999). Sediment production from forest roads in western Oregon. *Water Resources Research, 35,* 2561–2570.

Luo, P., He, B., Takara, K., Razafindrabe, B. H. N., Nover, D., & Yamashiki, Y. (2011). Spatiotemporal trend analysis of recent river water quality conditions in Japan. *Journal of Environmental Monitoring, 13,* 2819–2829.

Ma, X., Li, Y., Zhang, M., Zheng, F., & Du, S. (2011). Assessment and analysis of non-point source nitrogen and phosphorus loads in the Three Gorges Reservoir Area of Hubei Province, China. *Science of the Total Environment, 412–413,* 154–161.

Mann, H. B. (1945). Nonparametric tests against trend. *Econometrica, 13,* 245–259.

McMahon, G., Alexander, R. B., & Qian, S. (2003). Support of total maximum daily load programs using spatially referenced regression models. *Journal of Water Resources Planning and Management, 129,* 315–329.

Meade, R. H., Dunne, T., Richey, J. E., Santos, U. D. M., & Salati, E. (1985). Storage and remobilization of suspended sediment in the lower Amazon River of Brazil. *Science, 228*, 488.

Mizugaki, S., Onda, Y., Fukuyama, T., Koga, S., Asai, H., & Hiramatsu, S. (2008). Estimation of suspended sediment sources using 137Cs and 210Pbex in unmanaged Japanese cypress plantation watersheds in southern Japan. *Hydrological Processes, 22,* 4519–4531.

Nearing, M. A., Jetten, V., Baffaut, C., Cerdan, O., Couturier, A., Hernandez, M., et al. (2005). Modeling response of soil erosion and runoff to changes in precipitation and cover. *Catena, 61,* 131–154.

Nelson, E. J., & Booth, D. B. (2002). Sediment sources in an urbanizing, mixed land-use watershed. *Journal of Hydrology, 264,* 51–68.

Nielsen, J. P. (1999). *Record extension and streamflow statistics for the Pleasant River, Maine*. US Department of the Interior, US Geological Survey.

Preston, S. D., & US, G. S. (2009). *SPARROW modeling: Enhancing understanding of the nation's water quality*. US Department of the Interior, US Geological Survey.

Rajaee, T., Nourani, V., Zounemat-Kermani, M., & Kisi, O. (2011). River suspended sediment load prediction: Application of ANN and wavelet conjunction model. *Journal of Hydrologic Engineering, 16,* 613.

Ran, Q., Su, D., Li, P., & He, Z. (2012). Experimental study of the impact of rainfall characteristics on runoff generation and soil erosion. *Journal of Hydrology, 424,* 99–111.

Reckhow, K. H. (1994). Water quality simulation modeling and uncertainty analysis for risk assessment and decision making. *Ecological Modelling, 72,* 1–20.

Runkel, R. L., Crawford, C. G., Cohn, T. A., & US, G. S. (2004). *Load estimator (LOADEST): A FORTRAN program for estimating constituent loads in streams and rivers*. US Department of the Interior, US Geological Survey.

Sakamoto, Y., Ishiguro, M., & Kitagawa, G. (1986). *Akaike information criterion statistics*. New York: Springer.

Schwarz, G. E. (2008). A Preliminary SPARROW Model of Suspended Sediment for the Conterminous United States. U.S. Geological Survey Open-File Report 2008–1205, 7 pp. Retrieved June 2019, from https://pubs.usgs.gov/of/2008/1205/ofr2008-1205.pdf.

Schwarz, G. E., Hoos, A. B., Alexander, R. B., & Smith, R. A. (2006). *The SPARROW surface water-quality model: Theory, application, and user documentation*. USGS Techniques and Methods Report. Book 6, Chapter B3. USGS, Washington, DC.

Shumway, R. H., Azari, R. S., & Kayhanian, M. (2002). Statistical approaches to estimating mean water quality concentrations with detection limits. *Environmental Science and Technology, 36,* 3345–3353.

Smith, R. A., Schwarz, G. E., & Alexander, R. B. (1997). Regional interpretation of water-quality monitoring data. *Water Resources Research, 33,* 2781–2798.

Smith, V. H. (1982). The nitrogen and phosphorus dependence of algal biomass in lakes: An empirical and theoretical analysis. *Limnology and Oceanography, 27,* 1101–1112.

Somura, H., Takeda, I., Arnold, J. G., Mori, Y., Jeong, J., Kannan, N., et al. (2012). Impact of suspended sediment and nutrient loading from land uses against water quality in the Hii River basin, Japan. *Journal of Hydrology, 450,* 25–35.

Sprague, L. A., & Lorenz, D. L. (2009). Regional nutrient trends in streams and rivers of the United States, 1993–2003. *Environmental Science and Technology, 43,* 3430–3435.

Trimble, S. W. (1997). Contribution of stream channel erosion to sediment yield from an urbanizing watershed. *Science, 278,* 1442–1444.

Tu, J. (2011). Spatial and temporal relationships between water quality and land use in northern Georgia, USA. *Journal of Integrative Environmental Sciences, 8,* 151–170.

Vogel, R. M., & Stedinger, J. R. (1985). Minimum variance streamflow record augmentation procedures. *Water Resources Research, 21,* 715–723.

Wang, Y., He, B., Duan, W., Li, W., Luo, P., & Razafindrabe, B. (2016). Source apportionment of annual water pollution loads in river basins by remote-sensed land cover classification. *Water, 8,* 361.

Webb, B. W., Phillips, J. M., Walling, D. E., Littlewood, I. G., Watts, C. D., & Leeks, G. (1997). Load estimation methodologies for British rivers and their relevance to the LOIS RACS (R) programme. *Science of the Total Environment, 194,* 379–389.

Woli, K. P., Nagumo, T., Kuramochi, K., & Hatano, R. (2004). Evaluating river water quality through land use analysis and N budget approaches in livestock farming areas. *Science of the Total Environment, 329,* 61–74.

Wolman, M. G. (1967). A cycle of sedimentation and erosion in urban river channels. *Geografiska Annaler. Series A. Physical Geography, 49,* 385–395.

Yue, S., Pilon, P., & Cavadias, G. (2002). Power of the Mann–Kendall and Spearman's rho tests for detecting monotonic trends in hydrological series. *Journal of Hydrology, 259,* 254–271.